



# Advantages of integrating Brillouin microscopy in multimodal mechanical mapping of cells and tissues

Chenchen Handler<sup>1,a</sup>, Claudia Testi<sup>2,3,a</sup> and Giuliano Scarcelli<sup>2</sup>

## Abstract

Recent research has highlighted the growing significance of the mechanical properties of cells and tissues in the proper execution of physiological functions within an organism; alterations to these properties can potentially result in various diseases. These mechanical properties can be assessed using various techniques that vary in spatial and temporal resolutions as well as applications. Due to the wide range of mechanical behaviors exhibited by cells and tissues, a singular mapping technique may be insufficient in capturing their complexity and nuance. Consequently, by utilizing a combination of methods—multimodal mechanical mapping—researchers can achieve a more comprehensive characterization of mechanical properties, encompassing factors such as stiffness, modulus, viscoelasticity, and forces. Furthermore, different mapping techniques can provide complementary information and enable the exploration of spatial and temporal variations to enhance our understanding of cellular dynamics and tissue mechanics. By capitalizing on the unique strengths of each method while mitigating their respective limitations, a more precise and holistic understanding of cellular and tissue mechanics can be obtained. Here, we spotlight Brillouin microscopy (BM) as a noncontact, noninvasive, and label-free mechanical mapping modality to be coultized alongside established mechanical probing methods. This review summarizes some of the most widely adopted individual mechanical mapping techniques and highlights several recent multimodal approaches demonstrating their utility. We envision that future studies aim to adopt multimodal techniques to drive advancements in the broader realm of mechanobiology.

## Addresses

<sup>1</sup> Department of Mechanical Engineering, A. James Clark School of Engineering, University of Maryland, College Park, MD 20742, USA

<sup>2</sup> Fischell Department of Bioengineering, A. James Clark School of Engineering, University of Maryland, College Park, MD 20742, USA

<sup>3</sup> Center for Life Nano- and Neuro- Science, Istituto Italiano di Tecnologia, Viale Regina Elena 291, Rome 00161, Italy

Corresponding author: Scarcelli, Giuliano ([scarc@umd.edu](mailto:scarc@umd.edu))

<sup>a</sup> These authors contributed equally to this work.

Available online 11 March 2024

<https://doi.org/10.1016/j.ceb.2024.102341>

0955-0674/© 2024 Elsevier Ltd. All rights reserved.

## Introduction

In their natural environment, cells and tissues are subjected to various mechanical forces such as stretching, compression, and fluid shearing [1–4]. The ability to sense and respond to mechanical forces is governed by their stiffness or elastic modulus, which is vital for maintaining tissue integrity, guiding tissue development, and modulating gene expression and differentiation [1,2].

Under physiological conditions, cells tend to adapt to the mechanical characteristics of the surrounding environment; external mechanical cues are indeed translated into biochemical signals through intricate pathways, in a process called mechanotransduction [5]. A typical example of a crucial external physical cue sensed by cells through the mechanotransduction processes is constituted by the substrate stiffness of adherent cells, which deeply influences nuclear stiffness and determines cell fate. The nuclear architecture and stiffness of adherent cells grown on stiff substrates differ compared to cells grown on soft substrates [6,7]. In the same context, cells in suspension are mechanically different from their adherent counterpart, as a result of a different cytoskeletal organization [8,9]. The cytoskeleton also acts as a mechanosensitive element; disruptions in actin have been associated with changes in nuclear stiffness because of altered peripheral mechanical integrity [10]. Changes in cellular and tissue modulus are signatures of several human diseases, such as cardiovascular- [11], metabolic- [12], neurodegenerative-diseases [13], inflammation [11,14], and particularly metastatic cancers [15–20]. Metastatic cancer cells indeed exhibit reduced stiffness, a necessary adaptation for deforming and navigating through basement membranes [21]. Beyond cancer, single-point mutations in key proteins tuning chromatin relaxation in the nucleus are implicated in the rare genetic disease Kabuki Syndrome, correlating with

Current Opinion in Cell Biology 2024, 88:102341

This review comes from a themed issue on **Cell Dynamics 2023**

Edited by **Kandice Tanner** and **Anne Straube**

For complete overview of the section, please refer the article collection - [Cell Dynamics 2023](#)

increased nuclear stiffness in mesenchymal stem cells [22,23]. Mechanical alterations extend to the extracellular matrix, whose stiffness is affected in many pathologies as well, being strongly modified in fibrosis, for instance [24]. Furthermore, corneal and lens stiffness in the eyes change in conditions such as keratoconus [25] and presbyopia [26]. Stress granules, found in cells attributing to neurodegenerative diseases such as amyotrophic lateral sclerosis or Parkinson's, display higher stiffness and viscosity [27], stemming from the pathological accumulation of misfolded proteins that undergo a liquid-to-solid phase transition [28]. Additionally, increased arterial stiffness is associated with atherosclerosis plaque formation [29].

Thus, the exploration of rheological properties in cells and tissues under both physiological and pathological conditions not only holds potential for utilizing these properties as disease markers but also contributes to unraveling many mechanotransduction pathways that remain elusive. This has spurred the interest of many mechanical testing methods in the past three decades (Figure 1) [30–32].

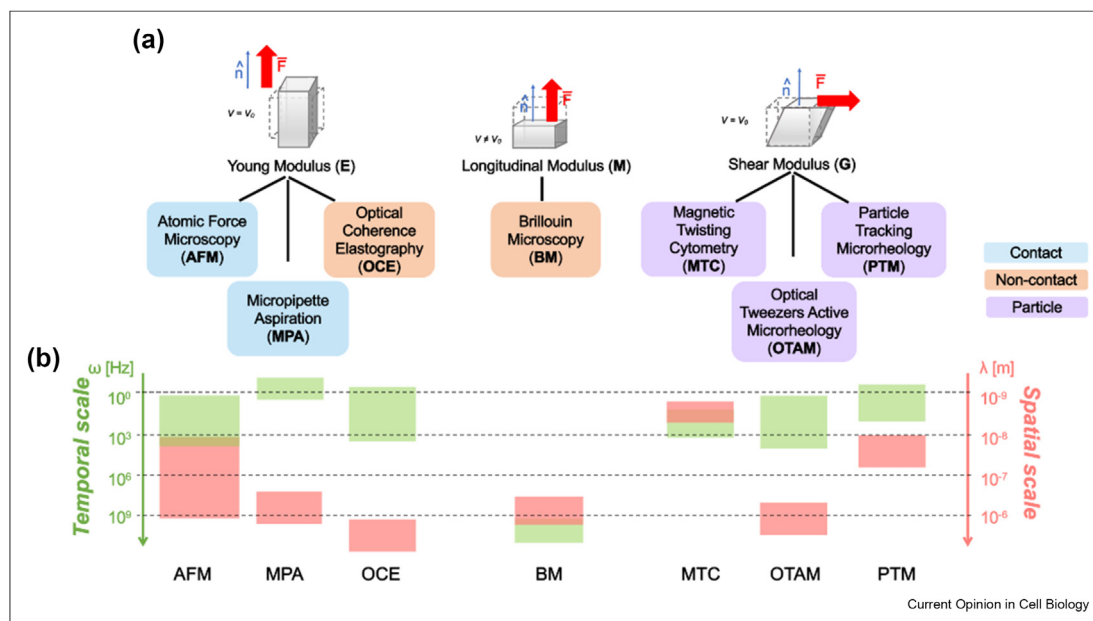
In this scenario, the varied spatiotemporal mechanical behavior of cells [33] and the intrinsic drawbacks of mechanical measurements applied to living materials have motivated correlative measurements that couple two or more methods. Historically, a single mechanical mapping technique is often combined with fluorescence

microscopy [18,19,34–37] to investigate both the molecular and mechanical properties of cells and tissues. However, relying on one technique to investigate biological mechanical properties may not be able to provide a complete characterization of complex behaviors. In this review, we will focus on tools that have been established for measuring cell and tissue mechanics. We will both highlight widely adopted techniques (Table 1) and focus on how pairing multiple techniques allows for mechanical characterization on different length and time scales (Figure 1). In the last few years, other innovative techniques have been proposed, such as micropatterned substrates [38], shear flow deformation cytometry [39], acoustic tweezers [40], microplate whole-cell microrheology [41], and many more [42–45]. In this review, we will focus on established techniques for which extensive literature on cellular and tissue applications exists.

## Overview of mechanical measurement methods

This section reviews the physical principles of several mechanical testing methods. It is important to note that other biomechanical techniques exist, but here we focus only on the ones most used in multimodal instruments for biological samples such as cells and tissues. The three mechanical moduli listed here represent different aspects of a material's deformation depending on the direction of the applied force  $F$  with respect to the axis  $n$

Figure 1



Overview of mechanical mapping techniques for biological materials. **a)** Mechanical moduli measured by contact-, noncontact-, and particle-based mapping techniques. **b)** Temporal (left, in green) and spatial (right, in red) scale of each technique in reference to 1 Å.

Table 1

## Overview of mechanical measurement techniques used in cells and tissues.

Category	Technique	Description/output	Spatial resolution in cells and tissues	Pros (+) and cons (-)
<b>Contact</b>	Atomic force microscopy ( <b>AFM-based microindentation</b> )	Measures Young's Modulus and cell adhesion.	>1 $\mu\text{m}$ , depending on the size of the tip for cell applications [49].	+ : Widely adopted and validated; gives high-resolution 2D E maps. - : Measurements performed only on the cell surface; relies on mathematical models to extract E [50].
	Micropipette aspiration ( <b>MPA</b> )	Measures adhesion, Young's Modulus, and viscoelasticity.	>200 nm, limited by camera pixel size [51,52].	+ : Direct mechanical measurement of global mechanical properties. - : Temporal resolution limited to camera framerate, low throughput.
<b>Particle</b>	Magnetic twisting cytometry ( <b>MTC</b> )	Measures shear modulus and viscoelasticity.	>5 nm [53,54].	+ : Utilizes beads to apply specific mechanical stress to the cytoskeleton via transmembrane mechanoreceptors; can probe many cells at a single time [54]. - : Limited frequency range, provides only punctual information of mechanical properties.
	Particle tracking microrheology ( <b>PTM</b> )	Measures shear viscoelastic modulus.	~10 nm, limited by camera [55].	+ : High spatial resolution - : Low throughput is invasive and provides only punctual information of mechanical properties.
	Optical tweezers active microrheology ( <b>OT/OTAM</b> )	Measures shear viscoelastic modulus.	On the order of single-digit $\mu\text{m}$ but highly dependent on bead size [56].	+ : Allows for single molecule manipulation. - : Cellular damage due to the focusing of high-powered lasers provides only punctual information of mechanical properties.
<b>Noncontact</b>	Brillouin microscopy ( <b>BM</b> )	Measures longitudinal modulus.	>1 $\mu\text{m}$ , diffraction limited [10].	+ : Gives high-resolution maps in 3D and is label-free and noninvasive. - : No established theoretical interpretation of mechanical signature.
	Optical coherence elastography ( <b>OCE</b> )	Measures local strains and Young's modulus.	>1–10 $\mu\text{m}$ , limited wavelength and speed of the traveling wave [57].	+ : Used in tissues, noninvasive. - : Limited cellular applications.

(Figure 1): *i*) Young's modulus ( $E$ ), which quantifies the material's ability to withstand tensions or compressions along the axis that does not change in volume; *ii*) longitudinal modulus ( $M$ ), which evaluates the material's ability to deform under tensions or compressions purely along the axis while changing its volume; and *iii*) shear modulus ( $G$ ), which characterizes the material's resistance to shear deformation. Another important note before introducing the various tests is that all the moduli in biological materials are strongly dependent on the frequency at which the mechanical perturbation is applied, a property called "viscoelasticity" [44,46,47]. All the aforementioned moduli are consequently frequency-dependent and complex functions. Their real and imaginary parts characterize the behavior of the material upon an external perturbation: the former represents the elastic response, while the latter represents the dissipative response. In the following, we will focus our attention on the real part of the moduli, dependent on sample stiffness, and we will not mention the imaginary part, related to sample viscosity, as the influence of viscosity on mechanotransduction and diseases has been less validated in the mechanobiology field compared to stiffness (although recent studies showed that cells are sensitive to viscosity cues as well [48]).

Techniques are divided into three categories (as in Table 1 and Figure 1): contact-based (in which the instrument physically touches the sample, possibly altering its mechanical response), particle-based (in which a particle, attached to the sample, is moved via optically or external magnetic or electric fields), and noncontact (in which the mechanical information is retrieved by exploiting light as a probe in a label-free manner).

*Atomic force microscopy* (AFM)-based indentations utilize a cantilever of calibrated stiffness with a sharp or rounded probe to apply a force to cells or tissues perpendicularly from above (Figure 2), working in the frequency range of Hz–kHz. The corresponding resistance to the deformation can be detected through the deflection of a laser reflected off the cantilever. By fitting the measured forces as a function of the vertical position of the probe, force-distance curves can be analyzed to quantify cellular stiffness [58] or elastic (effective Young's) modulus  $E$ . The fitting procedure, however, depends on a mathematical model to extract  $E$ ; any alterations to the theoretical framework can thus impact the obtained  $E$  values [50]. AFM is the gold-standard technique in mechanobiology as it has superb force sensitivity ( $\sim 10$  pN) [49,50,58] and accurate xy spatial resolution that might vary depending on the size and geometry of the bead; for example, when imaging bacteria's envelope structure, it has been found to be approximately 15 nm [49]. In order to retrieve information about the mechanical modulus in tissues and

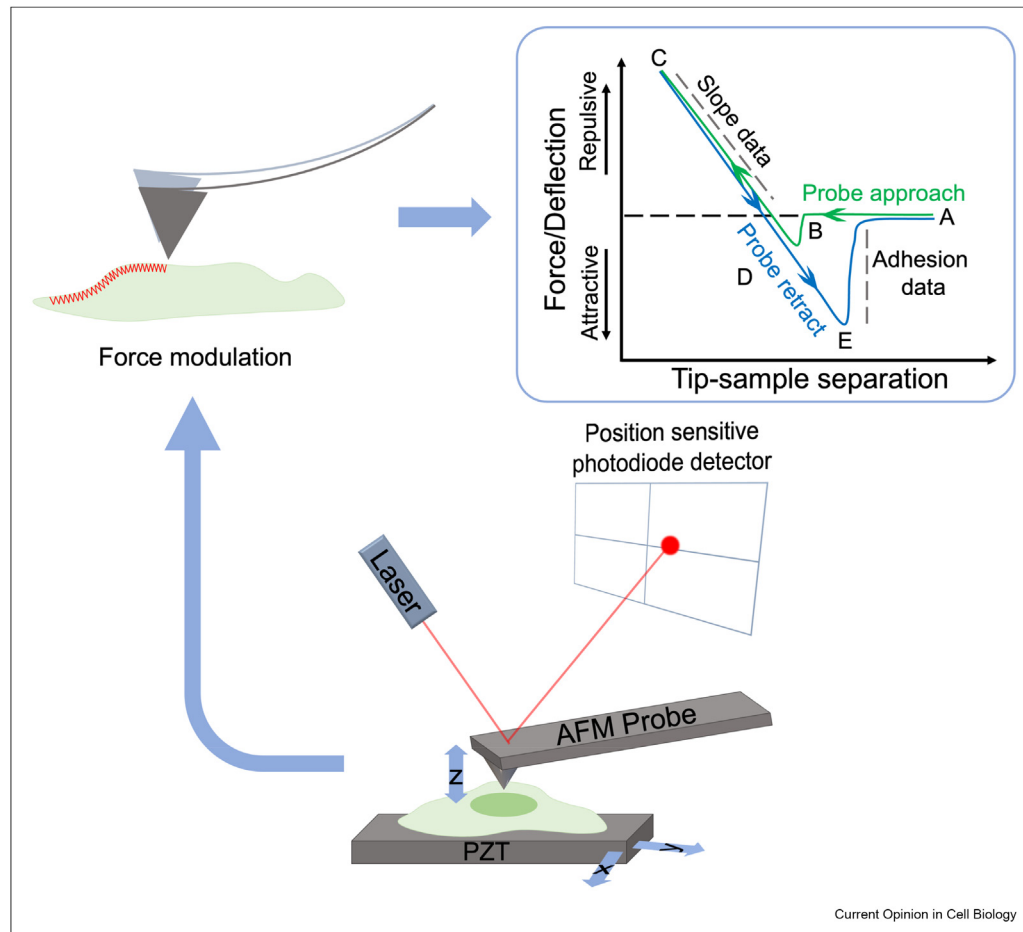
adherent cells, AFM-based indentation measurements are performed on the cell surface, and  $E$  values are averaged along the z-dimension of the cantilever. Here, it is used to generate 2D sub-micrometric mechanical maps of  $E$  along the surface [45,50]. The timescale of AFM is an important parameter to consider, as higher indentation speeds and higher indentation forces result in a higher elastic modulus [20,30] due to a lower retraction time. Varying these parameters can result in mechanical property measurements that differ by more than tenfold in the same sample [20,30].

*Micropipette aspiration* (MPA) involves immobilizing a suspended cell at the end of a glass pipette (typically ranging from 2 to 50  $\mu\text{m}$  in diameter), where a negative pressure is applied to deform and aspirate the cell membrane into the pipette at low frequencies (Hz) [32,51,52]. The resulting deformation is measured as a function of time with a spatial resolution of hundreds of nanometers. The degree of membrane deformation in response to the applied mechanical force is representative of the cell membrane's stiffness. Additionally, MPA can provide insight into cell adhesion [60] and viscoelasticity [61]. This technique is widely adopted due to its simplicity, but the lack of plate/capillary parallelism [62] and spatial resolution [52] contributes to inconsistencies across MPA readouts [34,37].

*Magnetic twisting cytometry* (MTC) requires using ferromagnetic beads (4–80  $\mu\text{m}$ ) on or inside the cell via surface integrin receptors or phagocytoses, respectively [46]. A controlled homogeneous magnetic field is applied via magnetic coils, which causes the beads to translocate and rotate. The shear modulus  $G$  and viscoelasticity at low frequencies (Hz–kHz [54]) of individual cells are related to the magnetic field applied (10–25 Gauss) [44,46,47], the bead-to-cell contact area (deformation), and the displacement of the beads. MTC can be used to apply both static and dynamic forces to cellular components such as the cytoskeleton and cell membrane [46,47], and it can probe many cells at a single time [54]. It can reach very high spatial resolution, up to 5 nm, when applied with other microscopic techniques such as fluorescence resonance energy transfer (FRET) [53] or stimulated emission depletion (STED) [54] microscopy, but the retrieved mechanical properties are only sensed locally, *i.e.* at a single point of a cell [45]. When using magnetic wires in a rotating magnetic field, the technique is called magnetic rotational spectroscopy [63].

*Particle tracking microrheology* (PTM) tracks the motion of small particles embedded within cells or tissues, such as nanoparticles [64], fluorescent [30], or magnetic [65] beads. High-frame rate video microscopy is used to analyze the trajectory of the beads due to the endogenous motions and vibrations of the sample, with up to  $\sim 10$  nm spatial resolution [55]. From the particle

Figure 2



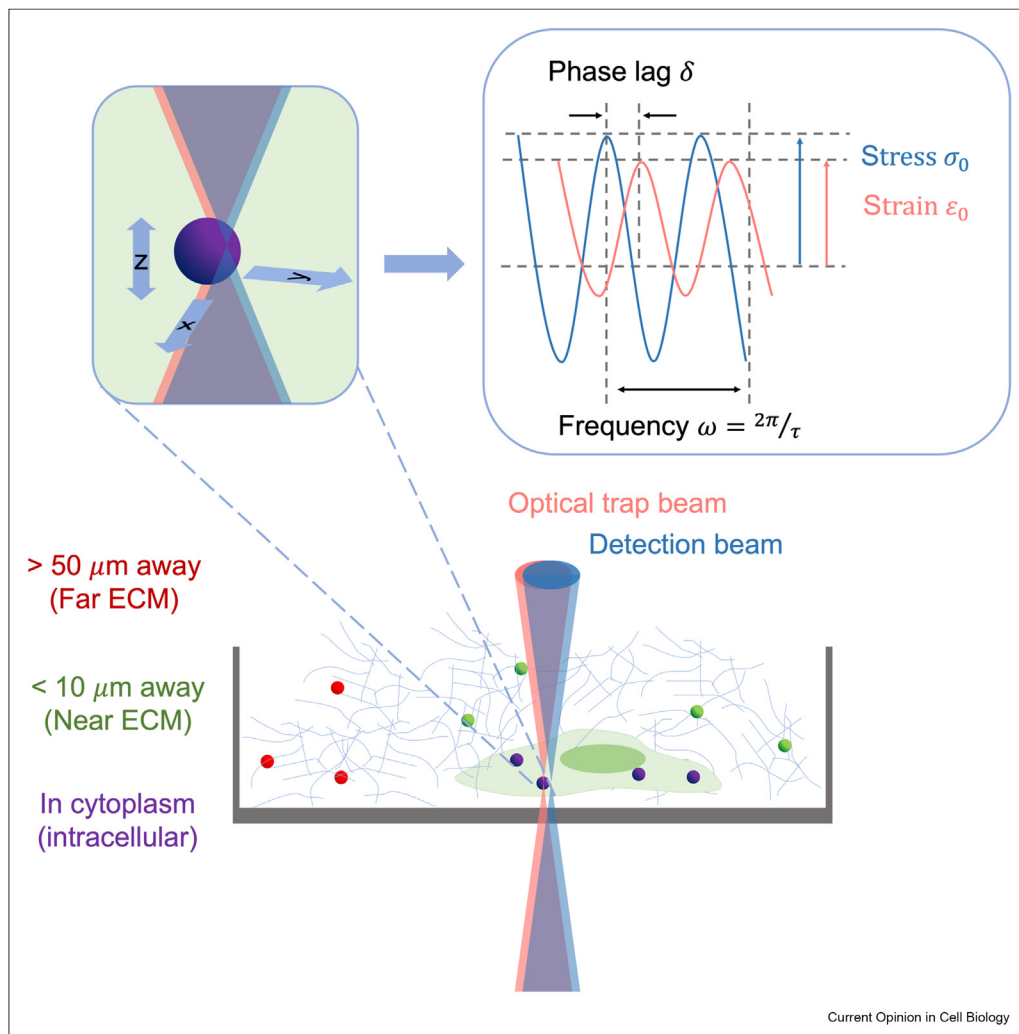
AFM is an example of a contact-based method demonstrating scan modes and force-deformation curve output. A sample is set on top of a PZT. Force modulation is a scan mode in which the cantilever tip experiences a force upon contact with the sample surface, and this force can be calculated as a function of tip-sample separation. The force/deflection curve illustrates an exemplary measurement using the force modulation mode, including interaction regions labeled A–E. A: no tip-sample interaction as the cantilever tip approaches the sample. B: the tip “snaps” into contact with the sample surface. C: tip is retracted but still in contact with the sample surface. D: cantilever deflects downwards due to attractive forces from the sample surface. E: tip detaches from the surface [59]. AFM, atomic force microscopy; PZT, piezoelectric scanner

trajectories, the mean-square displacement (MSD) [66] and the complex frequency-dependent shear viscoelastic modulus,  $G^*$ , can be obtained by using the MSD in the generalized Stokes-Einstein relation [67]. The retrieved mechanical properties are thus sensed only locally [45]. The frequency of  $G^*$  in the cell cytoplasm ranges from 0.1 to 100  $s^{-1}$  and is limited to the frame rate of the camera [68].

*Optical tweezers active microrheology* (OTAM) employs a highly focused laser beam to trap particles in *i*) the surrounding extracellular matrix (ECM) far from the cell ( $>50 \mu\text{m}$ ), *ii*) in the surrounding ECM close to the cell ( $<10 \mu\text{m}$ ), or *iii*) within the cytoplasm of the cell [69] (Figure 3). Active microrheology refers to monitoring the probe particle’s motion in response to external perturbation, in contrast to passive microrheology, which

involves observing the motion of the probe particle in response to thermal fluctuations. Sinusoidal oscillation of the laser beam causes trapped beads to apply local stresses to surrounding material, which yields local  $G^*$  over a wide range of frequencies (3–15,000 Hz) [7,69]. OTAM has been employed to assess the biomechanics of the nuclear cytoplasm [34,70] and cell–ECM coupling and homeostasis [69,71]. In cells, tracking single beads determines the rheological properties at the scale of the bead size ( $\sim 0.1\text{--}1 \mu\text{m}$ ), although this method may cause cellular damage due to the requirement for collimated high-powered laser beams [72], and the retrieved mechanical properties are only sensed locally [45]. Conversely, when performed on single molecules in solution, it can measure forces and displacements with accuracies within a few nanometers [73].

Figure 3



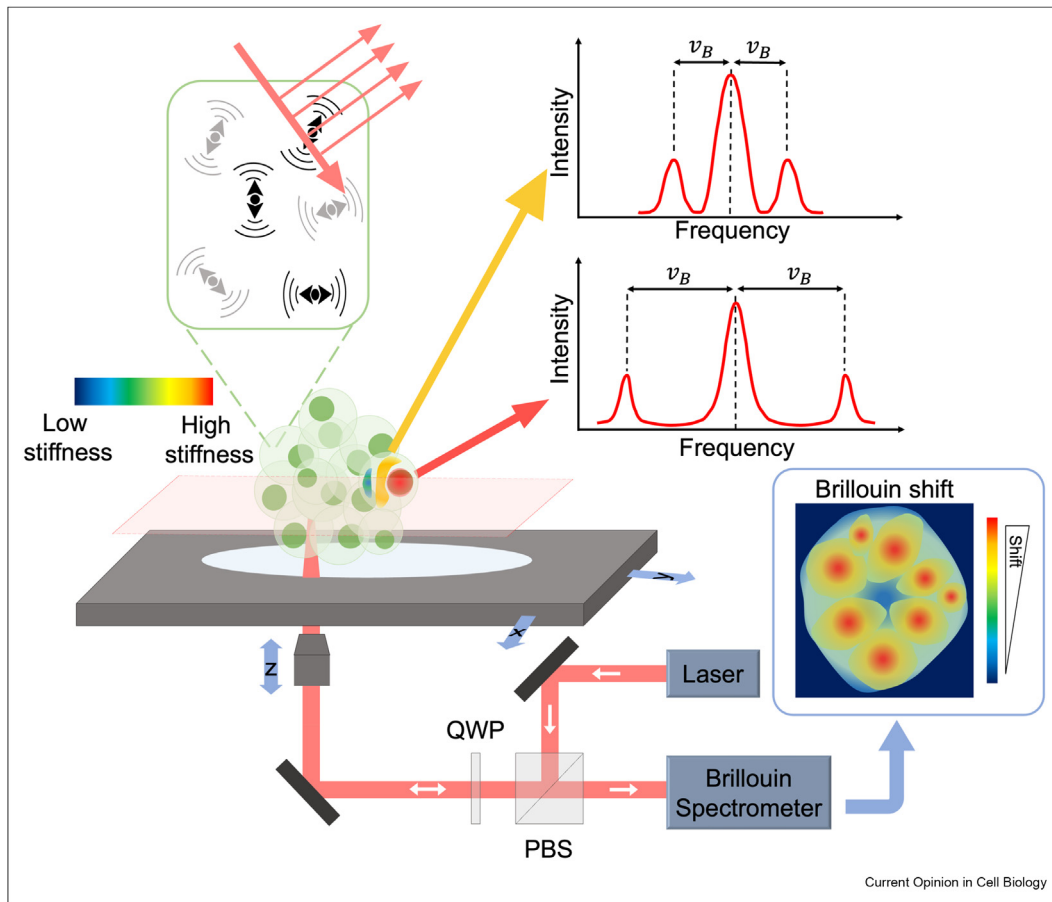
OTAM is an example of a particle-based method. Beads used in OTAM can be placed far from the cell and in the surrounding extracellular environment ( $>50 \mu\text{m}$ , red), near the cell ( $<10 \mu\text{m}$ , green), or intracellularly (purple). Figure adapted from J. R. Staunton et al. [69]. OTAM, optical tweezer active microrheology.

*Brillouin microscopy (BM)* is based on Brillouin scattering, where the incident photon interacts with acoustic phonons within the sample and introduces a frequency shift (Brillouin shift) to the scattered light [22,23,74] (Figure 4). Quantifying the Brillouin shift of the scattered light yields the elastic longitudinal modulus of the material [10] in the GHz regime. Using a confocal configuration, the spatial resolution of BM can achieve diffraction-limited axial and lateral resolution [75]. The Brillouin shift obtained in BM is representative of the longitudinal modulus of the material, which does not have a theoretically established correlation to Young's modulus for biological soft matter, though it is empirically correlated to Young's modulus [76]. BM provides diffraction-limited 3D maps of cell and tissue biomechanics in a noncontact, noninvasive, and label-free

manner, making it an advantageous technique for samples without physical access, such as 3D microenvironments [7] and microfluidics [77], or to retrieve the mechanical properties of intracellular compartments in 3D, such as the nucleus [10,23] or spheroids [78].

*Optical coherence elastography (OCE)* is based on inducing material deformation from a force excitation, for example, via an air puff, and using optical coherence tomography (OCT) to measure the spatially resolved deformation wave [57]. This wave velocity is used to map the local strains and the Young's modulus of the material at low frequencies (Hz–kHz) [79] with tens of microns of spatial resolution [57]. OCE has been widely used to quantify tissue mechanical properties [62] and less for cellular applications.

Figure 4



BM is an example of a noncontact-based method. Different regions of the cell are labeled with expected modulus (i.e. nucleus with high intrinsic stiffness, cytosol with lower intrinsic stiffness) and correlated to respective Brillouin signal outputs, with lower  $\nu_B$  output in the softer regions and higher  $\nu_B$  output in the high stiffness regions. Incoming photons from the laser beam interact with longitudinal phonons present in the sample (green box), thus giving rise to a Brillouin shift. The Brillouin shift map output (blue box) illustrates an exemplary XY cross-section (pink rectangle) of a spheroid. A Brillouin microscope is composed by a laser, a PBS and QWP to separate incoming from outgoing radiation, an objective to focalize the laser beam at the desired xyz location, and a high-resolution spectrometer that spatially disperses the frequencies and allows for the detection of a Brillouin spectrum (intensity vs frequency plots). BM, Brillouin microscopy; PBS, polarized beam splitter; QWP, quarter wave-plate

### Opportunity of multimodal mechanical mapping methods

While the methods listed above describe similar trends in mechanical characterization, measurement outputs may differ dramatically due to different timescales of sampling and data interpretation [1,35]. Multimodal mechanical assessment methods involve utilizing at least two different types of mechanical characterization techniques to assess mechanical properties to address different locations of the cell, different time or length scales, different environments, or a combination of these factors. Additionally, techniques can be used synergistically to counterbalance each other's shortcomings, i.e. one technique is able to assess mechanics at a global scale (as, for example, MPA), while the other technique is only able to locally survey mechanical properties (such as particle-based techniques). In this section, we aim to

highlight several recent papers utilizing multimodal mechanical mapping approaches.

#### Atomic force microscopy and micropipette aspiration

Experimental measurements of cellular responses often exhibit considerable variability attributed to factors like cell phenotypes, lineage, shape, and sourcing. Due to this variability, adequately describing a cell's mechanical behavior solely through *in vivo* testing may often become a formidable task, and elucidating the role of each subcomponent becomes even more difficult [80]. *Arduino et al.*\*\* used a finite element approach to model the mechanical response of cells undergoing AFM indentation and MPA; both revealed values of  $E$  in the MPa range. From AFM modeling, they found that the cytoskeleton is the most reactive, leading to nonuniform cell behavior. From the MPA model, they found that

changes in the ratio of cell diameter to pipette diameter influenced the aspiration length of the cell and that the cytoskeleton configuration contributes to structure involvement. Thus, the models used here allowed further insights into how varying the mechanical properties of single subcomponents affects overall cell behavior, which can be captured by one technique over another.

As previously noted, the values of elastic moduli obtained by AFM are highly influenced by the mathematical model employed for data analysis. In a study by *Daza et al.*, results on lymphocyte cells were derived by fitting AFM data with various models, ranging from simple to more sophisticated ones [81]. This approach yielded significantly divergent values for the elastic moduli, with much higher  $E$  values obtained by AFM compared to those determined by MPA ( $E_{AFM} = 1.9 \pm 0.1$  kPa vs  $E_{MPA} = 0.15 \pm 0.07$  kPa). While considering the finite size of cells helped diminish differences in the calculated elastic moduli, discrepancies persisted ( $E_{AFM} = 2.7 \pm 0.2$  kPa vs  $E_{MPA} = 0.5 \pm 0.03$  kPa). This may suggest that the localized nature of AFM measurements, in contrast with the more general character of MPA measurements, contributed to the observed variations.

#### Atomic force microscopy and optical tweezers

When applied to adherent cells, these techniques might provide complementary and seemingly discordant results as they are sensitive to different cellular properties. *Jokhadar et al.*\*\* aimed to investigate the effects of actin disruptors on endothelial cell mechanics using AFM and OT [82]. In the presence of actin disruptors, a significant increase in  $E$  was observed with AFM ( $\Delta_{AFM} = 0.87$  kPa), while a slight decrease in  $G$  was observed when measured with OT ( $\Delta_{OT} = -28$  pN/ $\mu$ m). The differences in stiffness measured with each technique can be attributed to the fact that different layers of cellular structures deform hierarchically and to varying degrees with increasing load forces: previous reports in fibroblasts [83] and neurons [84] also showed the same cell softening at small deformations (as the ones induced by OT) and a more solid-like behavior at larger deformations (as the ones induced by AFM). Thus, the combined responses of these different structures are observed in response to the large deformations applied during AFM experiments. On the other hand, actin disruptors were observed to induce effects on different scales of actin organization, which were only captured under small deformations using OT.

The same discrepancy between AFM and OT stiffness results has also been investigated by Mandal et al. [85], who exploited OT and AFM in bladder cells with an increasing cancer grade. The two techniques provided independent results: OT was exploited to probe only

intracellular mechanics with local high-resolution, while AFM was used in surface measurements to assess whole-cell mechanics. While both proved that high-grade cells were softer than low grade cells, AFM-retrieved stiffness values were two orders of magnitude larger than OT ( $E_{AFM} = 3$  kPa and  $E_{AFM} = 10$  kPa in RT112 and KU cells vs  $G_{OT} = 30$  Pa and  $G_{OT} = 25$  Pa in RT112 and KU cells), suggesting that AFM measurements, but not OT, were mostly dominated by cortical stiffness, as already noted by Jokhadar et al.

#### Magnetic twisting cytometry and atomic force microscopy

*Mallin et al.*\*\* sought to investigate the metastatic competency of polyan euploid cancer cell (PACC) state cells using MTC and AFM [47]. Cancer cells in the PACC state are characterized as cells that are non-dividing and enlarged due to increased genomic content as a stress-response behavior, a typical example of a mechanotransduction process. Here, *Mallin et al.* demonstrate that cells in the PACC state act as a hyper-elastic material that softens under tension (as proved by the MTC assay:  $\Delta_{PACC-CTRL} = -0.2$  Pa/nm, significant) while remaining unchanged under compression (as proved by the AFM:  $\Delta_{PACC-CTRL} = 0.1$  kPa, non-significant) [86]. Consequently, the apparent discrepancy in results prompted further downstream investigation into the functional deformability of PACC and non-PACC cells, revealing an interesting non-linear behavior of cancer cells that otherwise would have been missing.

#### Optical coherence elastography and optical tweezers active microrheology

*Sirotnin et al.*\*\* uniquely proposed employing OTAM to mechanically excite the cell membrane or organelles and phase-sensitive optical coherence microscopy (OCM) to measure the sample's response and associated mechanical properties [87]. OCM is a combination of optical coherence tomography and a confocal microscope, which allows for the highest resolution of OCE. Here, living red blood cells, yeast, and cancer cells were used to compare the two techniques. In the case of cancer cells, microspheres were employed at the cell surface, and OTAM was used to induce deformation. OCM was then applied to capture the response amplitudes of the microspheres corresponding to on-and-off OTAM cycles. The combination of these two techniques demonstrates label-free manipulation of the organelles of the cell while recording the organelle's position with nanometer accuracy due to the simultaneous use of coherence and confocal gates.

#### Multimodal techniques that include Brillouin microscopy

When physical access to the region of interest is limited, such as within tissues, spheroids, 3D microenvironments, or microfluidic channels, BM becomes the sole

valuable tool for capturing mechanical measurements that would otherwise be hard to obtain using conventional methods. However, as mentioned previously, the measured Brillouin shift is directly related to  $M$  (longitudinal modulus) at very high frequencies (1–10 GHz), far away from physiological timescales, and the retrieved  $M$  values are in the GPa range. As a result, for quantitative analysis, it is advisable to complement BM measurements with traditional methods as validation and calibration tools.

*Scarcelli et al.* and *Zhang et al.*\*\* employed this strategy by first measuring the average values of single cells under different perturbations with AFM and BM to extract an empirical correlation curve of Young's modulus *vs* longitudinal modulus; then they used the unique features of confocal BM and the much faster dual line-scanning Brillouin microscopy [78], respectively. Many other studies involve the correlation of longitudinal modulus values retrieved from BM in the GPa range with Young's modulus values retrieved from AFM in the kPa range, consistently revealing a robust empirical correlation in a log-log scale (i.e.  $\log(M/[Pa]) = a \cdot \log(E/[Pa]) + b$ , with  $a$  and  $b$  being sample-dependent [75,76,88,89]); however, a nontrivial relation between the two moduli has been found in a recent study involving fibrotic characterization over time in bladder tissues, in which the correlation between the two moduli changes as fibrosis progresses [24].

*Nikolić et al.*\*\* aimed to characterize the mechanical states of cancer cells in 2D and 3D ECM environments using BM and OTAM [7]. The combination of these techniques allowed for the comparative assessment of the microscale mechanical properties of two different moduli ( $G$  for OTAM,  $M$  for BM) at the same length scale ( $\sim 1 \mu\text{m}$ ) and in different frequency regimes (kHz for OTAM, GHz for BM). They found  $G$  values ranging from  $10 \cdot 10^3$  Pa with frequencies  $10^1$ – $10^4$  Hz, while  $M$  values ranged in the 2–2.1 GPa range at  $\sim 10$  GHz frequency. Both  $M$  and  $G$  increased with cytoskeletal changes such as actin upregulation, cross-linking, or branching, while they were not sensitive to 2D or 3D adhering environments. The observed good agreement of microscale properties between the two techniques validated Brillouin shift measurements and underlined that, despite the absence of an identified theoretical framework between the two moduli, there exists a shared dependence of  $M$  and  $G$  (or  $E$ ) on the underlying structural and biophysical factors within the samples.

*Roberts et al.*\*\* validated BM with an interferometric technique (confocal reflectance quantitative phase microscopy) to measure nuclear mechanics via membrane fluctuations and then used BM to characterize tumor cells during extravasation, reporting that metastatic cells had a lower modulus during the transmigration step [77].

At the tissue level, the most synergistic combination of BM is with OCE, which allows for rapid and direct quantitative measurements of tissue Young Modulus but is limited to backscattered configuration [90] in transparent tissues such as ocular tissues (i.e. cornea and lens). In contrast, BM can map the longitudinal modulus of transparent tissue with micro-scale resolution at any scattering angle [88]. *Ambekar et al.*\*\* devised a combined system of BM and OCE that allowed them to completely map the Young's modulus of the crystalline lens; here, the two techniques proved to reveal the same mechanical properties of gelatin gels under different conditions ( $E$  ranged 10–40 kPa,  $M$  ranged 2.10–2.45 GPa, a much lower dynamic range than  $E$  or  $G$ ) [91]. More recently, *Schumacher et al.*\*\* further refined the multimodal instrument of BM and OCE to evaluate in vivo lens biomechanics in the clinic in real time [26].

## Discussion and conclusion

In this review we aim to highlight recent advances in utilizing multimodal mechanical mapping approaches to measure the elastic modulus of cells and tissues.

The first part of this review consists of several widely adopted and gold-standard techniques for biological mechanical characterization that demonstrate, briefly, how each technique is used, the resulting outputs, and their respective advantages and limitations. The biggest limitation of contact-based techniques lies in the perturbations they induce in the specimen, which may alter its mechanical response. Additionally, techniques that require physical contact are impossible to employ in experiments that may require microfluidics or 3D microenvironments. On the other hand, all-optical methods such as OCE and BM have their shortcomings in terms of resolution (OCE) or the nonstandard nature of the modulus information (BM). We do think that when deciding which techniques to combine, researchers should strongly consider including noncontact mapping methods. While contact methods have set historical standards, it may be difficult to decouple the effects behind the induced forces via physical contact from the response to said physical contact. Additionally, contact-based methods have technical limitations, while noncontact methods may open more opportunities to explore cells and tissues in physiologically relevant settings such as 3D models and microfluidics. This status quo has motivated a shift towards combining multiple mechanical mapping techniques to cross-validate the results from individual techniques. Multimodal techniques may explore different time scales or length scales of measurement as well as local vs global assessments. Importantly, utilizing multiple techniques on the same sample has helped to elucidate the fact that different values of “modulus” are not contradictory; rather, they are the natural consequence of the physics of the specific testing method.

Our review focused on measurements of modulus, not forces, in biological samples. The past three decades have seen the development of several impressive force measuring methods, and the combination of force and modulus mapping is expected to be extremely powerful but has been rarely reported [92]. Our review also did not focus on the flourishing field of correlative techniques combining mechanical measurements with fluorescence microscopy [18,19,64,75,93,94]. The addition of fluorescence microscopy to a single-mode mechanical mapping technique is rapidly becoming standard operation and helps to unveil the connection between molecular and biomechanical behaviors.

Investigating rheological properties in cells and tissues, whether under physiological or pathological conditions, not only offers the prospect of employing the alteration of these properties as potential markers for diseases, but also aids in elucidating numerous elusive mechanotransduction pathways whose importance is growing in the biomedicine and mechanobiology fields. In this context, Brillouin microscopy emerges as a valuable tool capable of extracting a plethora of biophysical information of cells and tissues. Its potential is further amplified when employed in conjunction with established mechanical probing methods, offering a noncontact, noninvasive, and label-free approach for comprehensive mechanical mapping.

### Declaration of competing interest

The authors declare that they have no known competing financial interests or personal relationships that could have appeared to influence the work reported in this paper.

### Data availability

No data was used for the research described in the article.

### Acknowledgements

This research was funded by grants from ERC-2019-Synergy Grant (ASTRA, n. 855923); EIC-2022-PathfinderOpen (ivBM-4PAP, n. 101098989); Project "National Center for Gene Therapy and Drugs based on RNA Technology" (CN00000041) financed by NextGeneration EU PNRR MUR—M4C2—Action 1.4—Call "Potenziamento strutture di ricerca e creazione di "campioni nazionali di R&S" (CUP J33C22001130001) (to C.T.), by the National Science Foundation (DBI-1942003) and National Institutes of Health (R21CA258008, R01EY028666, R01EY030063). C.T. acknowledges financial support for this research by the Fulbright Research Scholar Program, which is sponsored by the U.S. Department of State and by the U.S.-Italy Fulbright Commission.

### References

Papers of particular interest, published within the period of review, have been highlighted as:

\*\* of outstanding interest

- Wirtz D, Konstantopoulos K, Searson PC: **The physics of cancer: the role of physical interactions and mechanical forces in metastasis.** *Nat Rev Cancer* Jul. 2011, **11**, <https://doi.org/10.1038/nrc3080>. Art. no. 7.
- Gayer CP, Basson MD: **The effects of mechanical forces on intestinal physiology and pathology.** *Cell Signal* Aug. 2009, **21**: 1237–1244, <https://doi.org/10.1016/j.cellsig.2009.02.011>.
- Tang X, *et al.*: **Mechanical force affects expression of an in vitro metastasis-like phenotype in HCT-8 cells.** *Biophys J* Oct. 2010, **99**:2460–2469, <https://doi.org/10.1016/j.bpj.2010.08.034>.
- Kumar S, Weaver VM: **Mechanics, malignancy, and metastasis: the force journey of a tumor cell.** *Cancer Metastasis Rev* Jun. 2009, **28**:113–127, <https://doi.org/10.1007/s10555-008-9173-4>.
- Di X, *et al.*: **Cellular mechanotransduction in health and diseases: from molecular mechanism to therapeutic targets.** *Signal Transduct Targeted Ther* Jul. 2023, **8**, <https://doi.org/10.1038/s41392-023-01501-9>. Art. no. 1.
- Yi B, Xu Q, Liu W: **An overview of substrate stiffness guided cellular response and its applications in tissue regeneration.** *Bioact Mater* Sep. 2022, **15**:82–102, <https://doi.org/10.1016/j.bioactmat.2021.12.005>.
- Nikolić M, Scarcelli G, Tanner K: **Multimodal microscale mechanical mapping of cancer cells in complex microenvironments.** *Biophys J* Oct. 2022, **121**:3586–3599, <https://doi.org/10.1016/j.bpj.2022.09.002>.  
Measured the response of intracellular mechanics of cancer cells in 2D and 3D to mimic in vivo extracellular matrix environments. Using Brillouin microscopy and optical tweezers, active microrheology can be used to map microscale cellular mechanics.
- Chan CJ, *et al.*: **Myosin II activity softens cells in suspension.** *Biophys J* Apr. 2015, **108**:1856–1869, <https://doi.org/10.1016/j.bpj.2015.03.009>.
- Maloney JM, *et al.*: **Mesenchymal stem cell mechanics from the attached to the suspended state.** *Biophys J* Oct. 2010, **99**: 2479–2487, <https://doi.org/10.1016/j.bpj.2010.08.052>.
- Zhang J, *et al.*: **Nuclear mechanics within intact cells is regulated by cytoskeletal network and internal nanostructures.** *Small* 2020, **16**, 1907688, <https://doi.org/10.1002/sml.201907688>.
- Mehta V, *et al.*: **Mechanical forces regulate endothelial-to-mesenchymal transition and atherosclerosis via an Alk5-Shc mechanotransduction pathway.** *Sci Adv* Jul. 2021, **7**:eabg5060, <https://doi.org/10.1126/sciadv.abg5060>.
- Zhu W, *et al.*: **PIEZO1 mediates a mechanothrombotic pathway in diabetes.** *Sci Transl Med* Jan. 2022, **14**:eabk1707, <https://doi.org/10.1126/scitranslmed.abk1707>.
- Hall CM, Moeendarbary E, Sheridan GK: **Mechanobiology of the brain in ageing and Alzheimer's disease.** *Eur J Neurosci* 2021, **53**:3851–3878, <https://doi.org/10.1111/ejn.14766>.
- Javier-Torrent M, Zimmer-Bensch G, Nguyen L: **Mechanical forces orchestrate brain development.** *Trends Neurosci* Feb. 2021, **44**:110–121, <https://doi.org/10.1016/j.tins.2020.10.012>.
- Reuten R, *et al.*: **Basement membrane stiffness determines metastases formation.** *Nat Mater* Jun. 2021, **20**, <https://doi.org/10.1038/s41563-020-00894-0>. Art. no. 6.
- Harada T, *et al.*: **Nuclear lamin stiffness is a barrier to 3D migration, but softness can limit survival.** *JCB (J Cell Biol)* Feb. 2014, **204**:669–682, <https://doi.org/10.1083/jcb.201308029>.
- Cross SE, Jin Y-S, Rao J, Gimzewski JK: **Nanomechanical analysis of cells from cancer patients.** *Nat Nanotechnol* Dec. 2007, **2**, <https://doi.org/10.1038/nnano.2007.388>. Art. no. 12.
- Weder G, *et al.*: **Increased plasticity of the stiffness of melanoma cells correlates with their acquisition of metastatic properties.** *Nanomedicine: nanotechnology, Biology and Medicine* Jan. 2014, **10**:141–148, <https://doi.org/10.1016/j.nano.2013.07.007>.
- Byfield FJ, Reen RK, Shentu T-P, Levitan I, Gooch KJ: **"Endothelial actin and cell stiffness is modulated by substrate stiffness in 2D and 3D,"** *Journal of Biomechanics*. **42**, no May 2009, **8**:1114–1119, <https://doi.org/10.1016/j.jbiomech.2009.02.012>.

20. Wullkopf L, *et al.*: **Cancer cells' ability to mechanically adjust to extracellular matrix stiffness correlates with their invasive potential, MBoC.** *29*, no Oct. 2018, **20**:2378–2385, <https://doi.org/10.1091/mbc.E18-05-0319>.
21. Alibert C, Goud B, Manneville J-B: **Are cancer cells really softer than normal cells?** *Biol Cell* 2017, **109**:167–189, <https://doi.org/10.1111/boc.201600078>.
22. Fasciani A, *et al.*: **MLL4-associated condensates counterbalance Polycomb-mediated nuclear mechanical stress in Kabuki syndrome.** *Nat Genet* Dec. 2020, **52**, <https://doi.org/10.1038/s41588-020-00724-8>. Art. no. 12.
23. Testi C, Fasciani A, Pontecorvo E, Gala F, Zippo A, Ruocco G: **MLL4 protein tunes chromatin compaction and regulates nuclear mechanical stress.** In *Optical elastography and tissue biomechanics VIII*. SPIE; Mar. 2021, 1164506, <https://doi.org/10.1117/12.2583238>.
24. Martinez-Vidal L, *et al.*: **Progressive alteration of murine bladder elasticity in actinic cystitis detected by Brillouin microscopy.** *Sci Rep* Jan. 2024, **14**, <https://doi.org/10.1038/s41598-023-51006-2>. Art. no. 1.
25. Scarcelli G, Besner S, Pineda R, Yun SH: **Biomechanical characterization of keratoconus corneas ex vivo with Brillouin microscopy.** *Invest Ophthalmol Vis Sci* Jul. 2014, **55**: 4490–4495, <https://doi.org/10.1167/iov.14-14450>.
26. Schumacher J, Schill AW, Singh M, Manns F, Larin KV, Scarcelli G: **Combining OCE and Brillouin microscopy to evaluate in vivo lens biomechanics in 3D.** In *Ophthalmic technologies XXXIII*. SPIE; Mar. 2023. PC123600N, <https://doi.org/10.1117/12.2649355>.
- A combination of optical coherence elastography and Brillouin microscopy system is used to derive depth-dependent elastic moduli in vivo using biomechanics. This is the first example of using this combination for investigating causes of lens stiffness in vivo for presbyopia.
27. Law JO, *et al.*: **A bending rigidity parameter for stress granule condensates.** *Sci Adv* May 2023, **9**:eadg0432, <https://doi.org/10.1126/sciadv.adg0432>.
28. Patel A, *et al.*: **A liquid-to-solid phase transition of the ALS protein FUS accelerated by disease mutation.** *Cell* Aug. 2015, **162**:1066–1077, <https://doi.org/10.1016/j.cell.2015.07.047>.
29. Stoka KV, *et al.*: **Effects of increased arterial stiffness on atherosclerotic plaque amounts.** *J Biomech Eng* May 2018, **140**, <https://doi.org/10.1115/1.4039175>. 0510071–05100710.
30. Guck J, Ananthakrishnan R, Mahmood H, Moon TJ, Cunningham CC, Käs J: **The optical stretcher: a novel laser tool to micromanipulate cells.** *Biophys J* Aug. 2001, **81**: 767–784, [https://doi.org/10.1016/S0006-3495\(01\)75740-2](https://doi.org/10.1016/S0006-3495(01)75740-2).
31. Radmacher M: **Measuring the elastic properties of biological samples with the AFM.** *IEEE Eng Med Biol Mag* Mar. 1997, **16**: 47–57, <https://doi.org/10.1109/51.582176>.
32. Hochmuth RM: **Micropipette aspiration of living cells.** *J Biomech* Jan. 2000, **33**:15–22, [https://doi.org/10.1016/S0021-9290\(99\)00175-X](https://doi.org/10.1016/S0021-9290(99)00175-X).
33. Learthrapun N, Zeng Z, Hajjarian Z, Bossuyt V, Nadkarni SK: **Speckle rheological spectroscopy reveals wideband viscoelastic spectra of biological tissues.** *bioRxiv* Jun. 10, 2023: 2023, <https://doi.org/10.1101/2023.06.08.544037>. 06.08.544037.
34. Vahabikashi A, *et al.*: **Nuclear lamin isoforms differentially contribute to LINC complex-dependent nucleocytoskeletal coupling and whole-cell mechanics.** *Proc Natl Acad Sci USA* Apr. 2022, **119**, e2121816119, <https://doi.org/10.1073/pnas.2121816119>.
35. Tsujita K, *et al.*: **Homeostatic membrane tension constrains cancer cell dissemination by counteracting BAR protein assembly.** *Nat Commun* Oct. 2021, **12**, <https://doi.org/10.1038/s41467-021-26156-4>. Art. no. 1.
36. Grady ME, Composto RJ, Eckmann DM: **Cell elasticity with altered cytoskeletal architectures across multiple cell types.** *J Mech Behav Biomed Mater* Aug. 2016, **61**:197–207, <https://doi.org/10.1016/j.jmbbm.2016.01.022>.
37. Efremov Yu M, Dokrunova AA, Efremenko AV, Kirpichnikov MP, Shaitan KV, Sokolova OS: **Distinct impact of targeted actin cytoskeleton reorganization on mechanical properties of normal and malignant cells.** *Biochim Biophys Acta Mol Cell Res* Nov. 2015, **1853**:3117–3125, <https://doi.org/10.1016/j.bbamcr.2015.05.008>. Part B.
38. Mandal K, Asnacios A, Goud B, Manneville J-B: **Mapping intracellular mechanics on micropatterned substrates.** *Proc Natl Acad Sci USA* Nov. 2016, **113**:E7159–E7168, <https://doi.org/10.1073/pnas.1605112113>.
39. Gerum R, *et al.*: **Viscoelastic properties of suspended cells measured with shear flow deformation cytometry.** *Elife* Sep. 2022, **11**, e78823, <https://doi.org/10.7554/eLife.78823>.
40. Yang S, *et al.*: **Acoustic tweezers for high-throughput single-cell analysis.** *Nat Protoc* Aug. 2023, **18**, <https://doi.org/10.1038/s41596-023-00844-5>. Art. no. 8.
41. Alibert C, *et al.*: **Multiscale rheology of glioma cells.** *Bio-materials* Aug. 2021, **275**, 120903, <https://doi.org/10.1016/j.biomaterials.2021.120903>.
42. Böhringer D, *et al.*: **Fiber alignment in 3D collagen networks as a biophysical marker for cell contractility.** *Matrix Biol* Dec. 2023, **124**:39–48, <https://doi.org/10.1016/j.matbio.2023.11.004>.
43. Kah D, *et al.*: **A low-cost uniaxial cell stretcher for six parallel wells.** *HardwareX* Apr. 2021, **9**, e00162, <https://doi.org/10.1016/j.ohx.2020.e00162>.
44. Wu P-H, *et al.*: **A comparison of methods to assess cell mechanical properties.** *Nat Methods* Jul. 2018, **15**, <https://doi.org/10.1038/s41592-018-0015-1>. Art. no. 7.
45. Regan K, *et al.*: **Multiscale elasticity mapping of biological samples in 3D at optical resolution.** *Acta Biomater* Dec. 2023, <https://doi.org/10.1016/j.actbio.2023.12.036>.
46. Hoffman BD, Massiera G, Van Citters KM, Crocker JC: **The consensus mechanics of cultured mammalian cells.** *Proc Natl Acad Sci USA* Jul. 2006, **103**:10259–10264, <https://doi.org/10.1073/pnas.0510348103>.
47. Mallin MM, *et al.*: **Cells in the polyan euploid cancer cell (PACC) state have increased metastatic potential.** *Clin Exp Metastasis* Jun. 2023, <https://doi.org/10.1007/s10585-023-10216-8>.
- Polyaneuploid cancer cells display increased metastatic traits such as heightened environment sensing and directional migration under chemotactic environments. Magnetic twisting cytometry and atomic force microscopy are used as mechanical testing methods.
48. Bera K, *et al.*: **Extracellular fluid viscosity enhances cell migration and cancer dissemination.** *Nature* Nov. 2022, **611**, <https://doi.org/10.1038/s41586-022-05394-6>. Art. no. 7935.
49. Dufrene YF, Viljoen A, Mignolet J, Mathelié-Guinlet M: **AFM in cellular and molecular microbiology.** *Cell Microbiol* 2021, **23**, e13324, <https://doi.org/10.1111/cmi.13324>.
50. Krieg M, *et al.*: **Atomic force microscopy-based mechanobiology.** *Nat Rev Phys* Jan. 2019, **1**, <https://doi.org/10.1038/s42254-018-0001-7>. Art. no. 1.
51. Berardi M, *et al.*: **Optical interferometry based micropipette aspiration provides real-time sub-nanometer spatial resolution.** *Commun Biol* May 2021, **4**, <https://doi.org/10.1038/s42003-021-02121-1>. Art. no. 1.
52. Liu X, Wang Y, Sun Y: **Cell contour tracking and data synchronization for real-time, high-accuracy micropipette aspiration.** *IEEE Trans Autom Sci Eng* Jul. 2009, **6**:536–543, <https://doi.org/10.1109/TASE.2009.2021356>.
53. Na S, Wang N: **Application of fluorescence resonance energy transfer and magnetic twisting cytometry to quantify mechanochemical signaling activities in a living cell.** *Sci Signal* Aug. 2008, **1**, <https://doi.org/10.1126/scisignal.134pl1>. pl1–pl1.
54. Zhang Y, *et al.*: **Interfacing 3D magnetic twisting cytometry with confocal fluorescence microscopy to image force responses in living cells.** *Nat Protoc* Jul. 2017, **12**, <https://doi.org/10.1038/nprot.2017.042>. Art. no. 7.

55. Crocker JC, Grier DG: **Methods of digital video microscopy for colloidal studies.** *J Colloid Interface Sci* Apr. 1996, **179**: 298–310, <https://doi.org/10.1006/jcis.1996.0217>.
56. Berghoff K, Gross W, Eisentraut M, Kress H: **Using blinking optical tweezers to study cell rheology during initial cell-particle contact.** *Biophys J* Aug. 2021, **120**:3527–3537, <https://doi.org/10.1016/j.bpj.2021.04.034>.
57. Wang S, Larin KV: **Shear wave imaging optical coherence tomography (SWI-OCT) for ocular tissue biomechanics.** *Opt. Lett., OL* Jan. 2014, **39**(1):41–44, <https://doi.org/10.1364/OL.39.000041>.
58. Hertz H. In *Ueber die Berührung fester elastischer Körper.*, 1882; Jan. 1882:156–171, <https://doi.org/10.1515/crll.1882.92.156>.
59. Mauer U, et al.: **Polymer characterization with the atomic force microscope.** *Polymer Science* 2013, <https://doi.org/10.5772/51060>. IntechOpen.
60. Ungai-Salánki R, et al.: **Single-cell adhesion strength and contact density drops in the M phase of cancer cells.** *Sci Rep* Sep. 2021, **11**, <https://doi.org/10.1038/s41598-021-97734-1>. Art. no. 1.
61. Tabatabaei M, Tafazzoli-Shadpour M, Khani MM: **Altered mechanical properties of actin fibers due to breast cancer invasion: parameter identification based on micropipette aspiration and multiscale tensegrity modeling.** *Med Biol Eng Comput* Mar. 2021, **59**:547–560, <https://doi.org/10.1007/s11517-021-02318-w>.
62. González-Bermúdez B, Guinea GV, Plaza GR: **Advances in micropipette aspiration: applications in cell biomechanics, models, and extended studies.** *Biophys J* Feb. 2019, **116**: 587–594, <https://doi.org/10.1016/j.bpj.2019.01.004>.
63. Dessard M, Manneville J-B, Berret J-F: **Cytoplasmic viscosity is a potential biomarker for metastatic breast cancer cells.** *bioRxiv* Jan. 09, 2024:2023, <https://doi.org/10.1101/2023.10.25.564072>. 10.25.564072.
64. Higgins G, Kim JE, Ferruzzi J, Abdalrahman T, Franz T, Zaman MH: **An exploratory study on the role of the stiffness of breast cancer cells in their detachment from spheroids and migration in 3D collagen matrices.** *bioRxiv* Apr. 16, 2022:2021, <https://doi.org/10.1101/2021.01.21.427639>. 01.21.427639.
65. Pokki J, Zisi I, Schulman E, Indana D, Chaudhuri O: **Magnetic probe-based microrheology reveals local softening and stiffening of 3D collagen matrices by fibroblasts.** *Biomed Microdevices* Apr. 2021, **23**:27, <https://doi.org/10.1007/s10544-021-00547-2>.
66. Tseng Y, Kole TP, Wirtz D: **Micromechanical mapping of live cells by multiple-particle-tracking microrheology.** *Biophys J* Dec. 2002, **83**:3162–3176, [https://doi.org/10.1016/S0006-3495\(02\)75319-8](https://doi.org/10.1016/S0006-3495(02)75319-8).
67. McGlynn JA, Wu N, Schultz KM: **Multiple particle tracking microrheological characterization: fundamentals, emerging techniques and applications.** *J Appl Phys* May 2020, **127**, 201101, <https://doi.org/10.1063/5.0006122>.
68. Hajjarian Z, Nadkarni SK: **Technological perspectives on laser speckle micro-rheology for cancer mechanobiology research.** *JBO* Sep. 2021, **26**, 090601, <https://doi.org/10.1117/1.JBO.26.9.090601>.
69. Staunton JR, So WY, Paul CD, Tanner K: **High-frequency microrheology in 3D reveals mismatch between cytoskeletal and extracellular matrix mechanics.** *Proc Natl Acad Sci USA* Jul. 2019, **116**:14448–14455, <https://doi.org/10.1073/pnas.1814271116>.
70. Ebata H, et al.: **Activity-dependent glassy cell mechanics I: mechanical properties measured with active microrheology.** *Biophys J* May 2023, **122**:1781–1793, <https://doi.org/10.1016/j.bpj.2023.04.011>.
71. Romani P, et al.: **Extracellular matrix mechanical cues regulate lipid metabolism through Lipin-1 and SREBP.** *Nat Cell Biol* Mar. 2019, **21**, <https://doi.org/10.1038/s41556-018-0270-5>. Art. no. 3.
72. Robertson-Anderson RM: **Optical tweezers microrheology: from the basics to advanced techniques and applications.** *ACS Macro Lett* Aug. 2018, **7**:968–975, <https://doi.org/10.1021/acsmacrolett.8b00498>.
73. Mukherjee C, Kundu A, Dey R, Banerjee A, Sengupta K: **Active microrheology using pulsed optical tweezers to probe viscoelasticity of laminin A.** *Soft Matter* Jul. 2021, **17**:6787–6796, <https://doi.org/10.1039/D1SM00293G>.
74. Brillouin L: **Diffusion de la lumière et des rayons X par un corps transparent homogène - influence de l'agitation thermique.** *Ann Phys* 1922, **9**, <https://doi.org/10.1051/anphys/192209170088>. Art. no. 17.
75. Scarcelli G, Yun SH: **Confocal Brillouin microscopy for three-dimensional mechanical imaging.** *Nat Photonics* Jan. 2008, **2**, <https://doi.org/10.1038/nphoton.2007.250>. Art. no. 1.
76. Scarcelli G, Kim P, Yun SH: **In vivo measurement of age-related stiffening in the crystalline lens by Brillouin optical microscopy.** *Biophys J* Sep. 2011, **101**:1539–1545, <https://doi.org/10.1016/j.bpj.2011.08.008>.
77. Roberts AB, et al.: **Tumor cell nuclei soften during trans-endothelial migration.** *J Biomech* May 2021, **121**, 110400, <https://doi.org/10.1016/j.jbiomech.2021.110400>.  
Investigated tumor cells transmigrating on an in vitro collagen gel platform using Brillouin microscopy and confocal reflectance quantitative phase microscopy. One of the first examples of utilizing two completely non-contact based mechanical probing methods in cells.
78. Zhang J, Nikolic M, Tanner K, Scarcelli G: **Rapid biomechanical imaging at low irradiation level via dual line-scanning Brillouin microscopy.** *Nat Methods* May 2023, **20**, <https://doi.org/10.1038/s41592-023-01816-z>. Art. no. 5.  
Application of dual line-scanning Brillouin microscopy (dLSMB) and atomic force microscopy in measuring the mechanical properties of cancer cells. The acquisition speed of dLSMB is 1 ms per pixel in biological samples and is more than one order of magnitude faster than current state-of-the-art spontaneous confocal or stimulated setups.
79. Zaitsev VY, et al.: **Strain and elasticity imaging in compression optical coherence elastography: the two-decade perspective and recent advances.** *J Biophot* 2021, **14**, e202000257, <https://doi.org/10.1002/jbio.202000257>.
80. Arduino A, Pettenuzzo S, Berardo A, Salomoni VA, Majorana C, Carniel EL: **A continuum-tensegrity computational model for chondrocyte biomechanics in AFM indentation and micropipette aspiration.** *Ann Biomed Eng* Dec. 2022, **50**:1911–1922, <https://doi.org/10.1007/s10439-022-03011-1>.  
Analyzing the mechanical response of how cellular subcomponents contribute to overall mechanical behavior using a continuous-tensegrity finite element model, including micropipette aspiration and atomic force microscopy.
81. Daza R, et al.: **Comparison of cell mechanical measurements provided by atomic force microscopy (AFM) and micropipette aspiration (MPA).** *J Mech Behav Biomed Mater* Jul. 2019, **95**: 103–115, <https://doi.org/10.1016/j.jmbm.2019.03.031>.
82. Jokhadar ŠZ, Iturri J, Toca-Herrera JL, Derganc J: **Cell stiffness under small and large deformations measured by optical tweezers and atomic force microscopy: effects of actin disruptors CK-869 and jasplakinolide.** *J Phys D Appl Phys* Jan. 2021, **54**, 124001, <https://doi.org/10.1088/1361-6463/abd0ae>.  
Jasplakinolide and CK-869 are used as cytoskeleton-disrupting drugs in human umbilical vein endothelial cells. Optical tweezers and atomic force microscopy are used to investigate drug effects on cellular mechanics.
83. Ayala YA, et al.: **Effects of cytoskeletal drugs on actin cortex elasticity.** *Exp Cell Res* Feb. 2017, **351**:173–181, <https://doi.org/10.1016/j.yexcr.2016.12.016>.
84. Amin L, Ercolini E, Shahapure R, Migliorini E, Torre V: **The role of membrane stiffness and actin turnover on the force exerted by DRG lamellipodia.** *Biophys J* Jun. 2012, **102**:2451–2460, <https://doi.org/10.1016/j.bpj.2012.04.036>.
85. Mandal K, et al.: **Role of a kinesin motor in cancer cell mechanics.** *Nano Lett* Nov. 2019, **19**:7691–7702, <https://doi.org/10.1021/acs.nanolett.9b02592>.

86. Nguyen H-D, Huang S-C: **The uniaxial stress–strain relationship of hyperelastic material models of rubber cracks in the platens of papermaking machines based on nonlinear strain and stress measurements with the finite element method.** *Materials* Jan. 2021, **14**, <https://doi.org/10.3390/ma14247534>. Art. no. 24.
87. Sirotnin MA, Romodina MN, Lyubin EV, Soboleva IV, Fedyanin AA: **Single-cell all-optical coherence elastography with optical tweezers.** *Biomed. Opt. Express, BOE* Jan. 2022, **13**(1):14–25, <https://doi.org/10.1364/BOE.444813>.  
Developed a novel label-free, single-cell, and all-optical coherence elastography method in combination with optical tweezers and phase-sensitive optical coherence microscopy. Technique demonstrated on red blood cells, yeast, and cancer cells as a tool for studying cellular and subcellular mechanics in vivo.
88. Besner S, Scarcelli G, Pineda R, Yun S-H: **In vivo Brillouin analysis of the aging crystalline lens.** *Invest Ophthalmol Vis Sci* Oct. 2016, **57**:5093–5100, <https://doi.org/10.1167/iov.16-20143>.
89. Weber IP, Yun SH, Scarcelli G, Franze K: **The role of cell body density in ruminant retina mechanics assessed by atomic force and Brillouin microscopy.** *Phys Biol* Nov. 2017, **14**, 065006, <https://doi.org/10.1088/1478-3975/aa6d18>.
90. Wu C, *et al.*: **Assessing age-related changes in the biomechanical properties of rabbit lens using a coaligned ultrasound and optical coherence elastography system.** *Invest Ophthalmol Vis Sci* Feb. 2015, **56**:1292–1300, <https://doi.org/10.1167/iov.14-15654>.
91. Ambekar YS, *et al.*: **Multimodal quantitative optical elastography of the crystalline lens with optical coherence elastography and Brillouin microscopy.** *Biomed. Opt. Express, BOE* Apr. 2020, **11**(4):2041–2051, <https://doi.org/10.1364/BOE.387361>.  
Optical coherence elastography and Brillouin microscopy were used to investigate the relationship between Young's moduli and longitudinal moduli in tissue mimicking gelatin phantoms and ex-vivo porcine crystalline lenses. The combination of the two techniques is used to overcome the drawbacks of individual modalities.
92. Coppola S, Schmidt T, Ruocco G, Antonacci G: **Quantifying cellular forces and biomechanical properties by correlative micropillar traction force and Brillouin microscopy.** *Biomed Opt Express* May 2019, **10**(5):2202–2212, <https://doi.org/10.1364/BOE.10.002202>.
93. Molter CW, Muszynski EF, Tao Y, Trivedi T, Clouvel A, Ehrlicher AJ: **Prostate cancer cells of increasing metastatic potential exhibit diverse contractile forces, cell stiffness, and motility in a microenvironment stiffness-dependent manner.** *Front Cell Dev Biol* 2022, **10** [Online]. Available: <https://www.frontiersin.org/articles/10.3389/fcell.2022.932510>. Accessed 13 June 2023.
94. Efremov YM, *et al.*: **Correlation of plasma membrane microviscosity and cell stiffness revealed via fluorescence-lifetime imaging and atomic force microscopy.** *Cells* Jan. 2023, **12**, <https://doi.org/10.3390/cells12212583>. Art. no. 21.